Biochimica et Biophysica Acta 1847 (2015) 418–428

Contents lists available at ScienceDirect

Biochimica et Biophysica Acta

journal homepage: www.elsevier.com/locate/bbabio

Altered p53 and NOX1 activity cause bioenergetic defects in a SCA7 polyglutamine disease model

Abiodun Ajayi, Xin Yu, Carolina Wahlo-Svedin, Galateia Tsirigotaki, Victor Karlström, Anna-Lena Ström *

Department of Neurochemistry, Stockholm University, SE-106 91 Stockholm, Sweden

ARTICLE INFO

Article history:
Received 5 September 2014
Received in revised form 12 December 2014
Accepted 26 January 2015
Available online 31 January 2015

Keywords:
Neurodegeneration
NADPH oxidase
Oxidative phosphorylation
Metabolism
p53

ABSTRACT

Spinocerebellar ataxia type 7 (SCA7) is one of the nine neurodegenerative disorders caused by expanded polyglutamine (polyQ) domains. Common pathogenic mechanisms, including bioenergetics defects, have been suggested for these so called polyQ diseases. However, the exact molecular mechanism(s) behind the metabolic dysfunction is still unclear. In this study we identified a previously unreported mechanism, involving disruption of p53 and NADPH oxidase 1 (NOX1) activity, by which the expanded SCA7 disease protein ATXN7 causes metabolic dysregulation. The NOX1 protein is known to promote glycolytic activity, whereas the transcription factor p53 inhibits this process and instead promotes mitochondrial respiration. In a stable inducible PC12 model of SCA7, p53 and mutant ATXN7 co-aggregated and the transcriptional activity of p53 was reduced, resulting in a 50% decrease of key p53 target proteins, like AIF and TIGAR. In contrast, the expression of NOX1 was increased approximately 2 times in SCA7 cells. Together these alterations resulted in a decreased respiratory capacity, an increased reliance on glycolysis for energy production and a subsequent 20% reduction of ATP in SCA7 cells. Restoring p53 function, or suppressing NOX1 activity, both reversed the metabolic dysfunction and ameliorated mutant ATXN7 toxicity. These results hence not only enhance the understanding of the mechanisms causing metabolic dysfunction in SCA7 disease, but also identify NOX1 as a novel potential therapeutic target in SCA7 and possibly other polyQ diseases.

1. Introduction

Spinocerebellar ataxia type 7 (SCA7) is one of the nine neurodegenerative disorders caused by expanded polyglutamine (polyQ) domains; for review see [1]. These so called polyQ diseases are characterized by intracellular aggregation of the expanded polyglutamine protein and common toxic gain-of-function mechanisms have been suggested. However, the exact toxic mechanism(s) is still unclear and the sequence surrounding the polyQ tract is believed to modulate the toxicity and contribute to the disease specific pattern of neuronal death in each disease [1–3]. In SCA7, the polyQ region is situated in ataxin-7 (ATXN7), a protein implicated in regulation of cytoskeleton stability and STAGA-(SPT3-TAF(II)31-GCN5L acetylase) mediated gene transcription [4–6]. Despite the widespread expression of ATXN7, mainly cerebellar, brainstem and retinal neurons are affected in SCA7 [7].

Oxidative stress, a situation where the levels of free radicals exceed the capacity of the cell's endogenous anti-oxidant systems, has been implicated in the pathology of polyglutamine diseases [1,8]. Recently, we and others have linked enhanced production of reactive oxygen species (ROS) by transmembrane NADPH oxidase (NOX) enzymes to the oxidative stress and toxicity in polyQ disease [9–12]. Under normal physiological conditions NOX enzymes generate low, local levels of superoxide, thereby regulating a number of redox-sensitive intracellular signaling molecules like phosphatases, transcription factors and ion channels [8]. To date, seven NOX family members, NOX1-5 and DUOX1-2, have been described and several of these are expressed in neurons [8,13,14]. However, the physiological role of the different NOX enzymes in the nervous system and how dys-regulation of these enzymes occurs and contributes to neurodegeneration are still largely unclear [8].

Besides oxidative stress, metabolic alterations and energy deficits have also been implicated in polyglutamine pathology [1,15]. Although some energy can be produced in the cytoplasm by glycolysis, i.e. the conversion of glucose into pyruvate, most ATP is generated when products of the tricarboxylic acid cycle (TCA), fatty acid and amino acid oxidation are used by mitochondria during oxidative phosphorylation (OxPhos) [16,17]. At the mitochondrial inner membrane, transfer of electrons from NADH and succinate to oxygen via mitochondrial complexes I–IV generates an electrochemical membrane gradient, which is

Abbreviations: ATXN7, ataxin-7; ETC, electron transport chain; HD, Hungtinton's disease; NOX, Nadph oxidase; OxPhos, oxidative phosphorylation; PolyQ, polyglutamine; SCA7, spinocerebellar ataxia type 7

* Corresponding author. Tel.: +46 8 161267; fax: +46 8 161371.
E-mail addresses: ajayi.abiodun@neurochem.su.se (A. Ajayi), xin.yu@neurochem.su.se (X. Yu), carro85@hotmail.com (C. Wahlo-Svedin), tsirigo3@hotmail.com (G. Tsirigotaki), victor.karlstrom@gmail.com (V. Karlström), anna-lena.strom@neurochem.su.se (A.-L. Ström).

http://dx.doi.org/10.1016/j.bbabio.2015.01.012
0005-2728/

subsequently used to drive the production of ATP by mitochondrial complex V. In the presence of oxygen, most cells primarily convert the pyruvate produced by glycolysis into acetyl-CoA, which then enters the TCA and OxPhos. Abnormal glucose metabolism, as well as altered TCA activity, has been reported in polyQ disease models and patients; for review see [15,18]. At the cellular level, the major cause of the metabolic alterations and energy deficiency appears to be mitochondrial abnormalities [15,19–21]. In SCA7 patients, abnormal mitochondria morphology, reduced electron transport chain activity, metabolic acidosis, as well as poor weight gain have been reported [19,22]. However, the exact mechanisms behind the mitochondrial damage and metabolic dysregulation in SCA7 and other polyQ diseases are still largely unclear.

The redox-sensitive transcription factor p53 plays a critical role in maintaining the integrity of mitochondria and oxidative phosphorylation [23,24]. Key p53 target genes, important for mitochondrial OxPhos, include AIF (apoptosis-inducing factor) and SCO2 (synthesis of cytochrome c oxidase) [23,24]. In contrast to promoting OxPhos, the overall effect of p53 on glycolysis is repressive [23,24]. This repressive effect is mediated through negative regulation of glucose transporter (GLUT) expression and p53-mediated induction of TIGAR (p53-inducible glycolysis and apoptosis regulator), which diverts glucose catabolism to the pentose-phosphate pathway (PPP) [23,24].

In this study, we for the first time show that the polyQ expanded ATXN7 disrupts the metabolic regulatory function of p53 and results in altered levels of AIF, TIGAR and GLUT1. In turn, this results in reduced mitochondrial respiration, a higher dependence on glycolysis and reduced ATP levels. Moreover, we showed that the NOX1 activity is specifically enhanced and is essential to sustain the metabolic dysregulation and toxicity in SCA7 cells.

2. Materials and methods

2.1. Cell culture and plasmid transfections

The generation and characterization of Tet-off inducible FLQ10 and FLQ65 PC12 cell lines, expressing C-terminal GFP tagged ATXN7 with

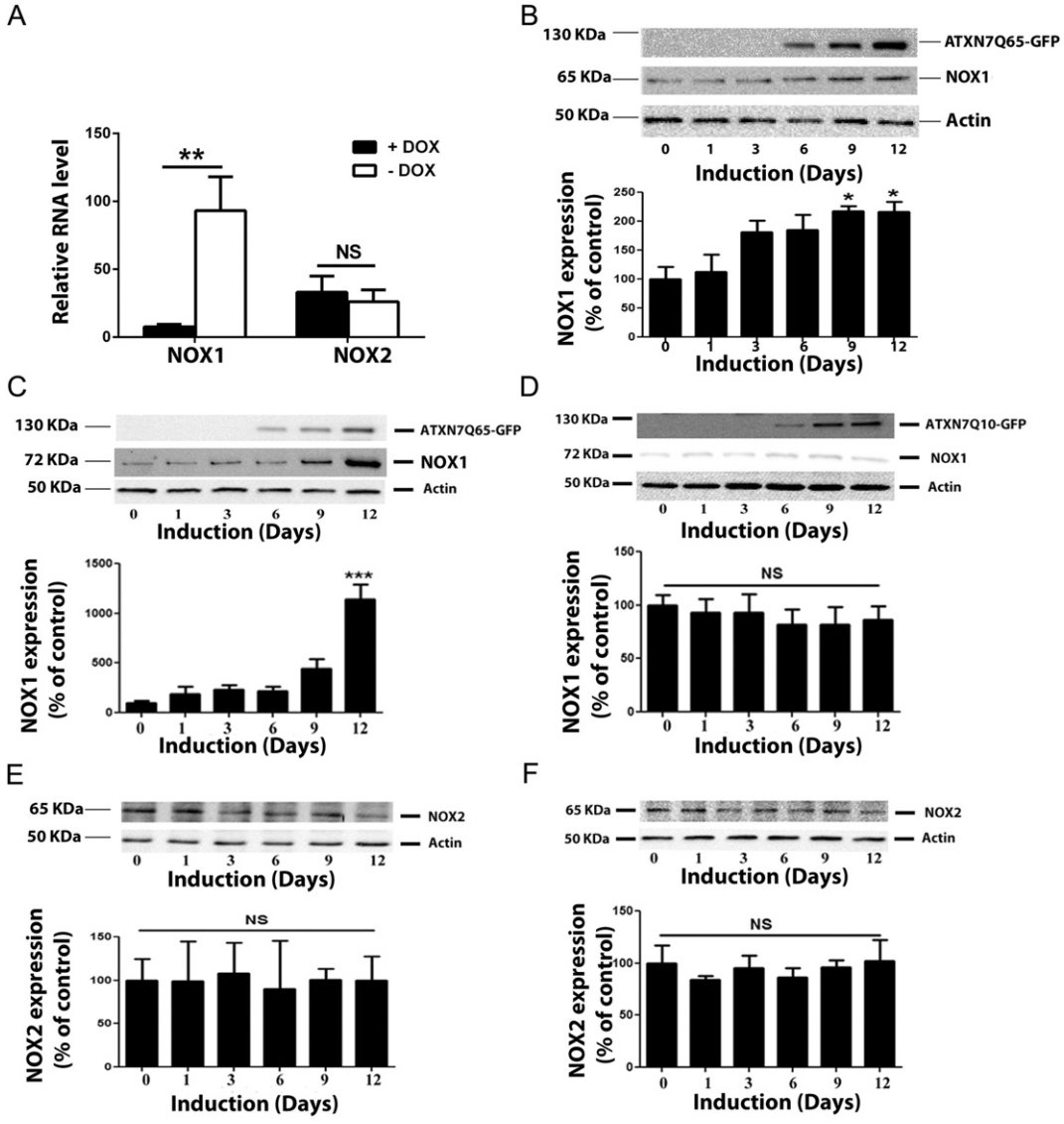

Fig. 1. Mutant ATXN7 causes up-regulation of NOX1, but not NOX2 expression. (A) Analysis of NOX1 and 2 mRNA levels in control, i.e. non-induced FLQ65 (+Dox) cells, or FLQ65 cells induced (−Dox) to express mutant GFP-tagged ATXN7 with 65 glutamines (ATXN7Q65-GFP) for 12 days. Removal of doxycycline (Dox) from the media induces ATXN7 expression. (B) Expression analysis of the 65 kDa NOX1 form in non-induced or FLQ65 cells induced to express mutant ATXN7 for the indicated number of days, using an antibody from Abcam. (C) Analysis of the 75 kDa NOX1 form, detected with an antibody from Sigma, in FLQ65 cells grown and induced as in B. (D) Expression of the 75 kDa NOX1 form in non-induced or FLQ10 cells induced to express wild-type GFP-tagged ATXN7 with 10 glutamines (ATXN7Q10-GFP). (E) NOX2 expression in FLQ65 cells grown and induced as in B. (F) NOX2 expression in FLQ10 cells grown as in B. Actin was used as loading control and for normalizations. All data are shown as means ± SEM from at least three independent experiments. * $p < 0.05$, ** $p < 0.01$, *** $p < 0.001$.

10 (ATXN7Q10-GFP) or 65 (ATXN7Q65-GFP) glutamines have been described previously [9,25]. The expression of ATXN7 in these rat neuronal-like cells is induced by the removal of doxycycline (Dox) from the culture media. Cells were grown at 37 °C and 5% CO_2, in DMEM (Invitrogen) supplemented with 10% horse serum (Invitrogen), 5% Tet System Approved fetal bovine serum (PAA), 100 μg/ml G418 (Invitrogen), 100 units/ml penicillin G sodium, 100 μg/ml streptomycin sulphate (Invitrogen), 100 μg/ml hygromycin (Invitrogen) and when desired 1 μg/ml Dox (Sigma).

Human HeLa cells were grown at 37 °C and 5% CO_2, in DMEM (Invitrogen) supplemented with 10% fetal bovine serum (Promega) and 100 units/ml penicillin G sodium. For HeLa transfections, plasmids FLQ10, FLQ65, TrQ10 and TrQ65, expressing FLAG-tagged full-length or truncated ATXN7 with 10 or 65 glutamines, respectively were used [26]. Cells were transfected at 50–80% confluency using Lipofectamine 2000 (Invitrogen), following the manufacturer's recommendations.

2.2. NOX1 knock-down and treatments

Stable PC12 cell lines were transfected with either non-targeting control small interfering si(RNA) or NOX1-specific siRNA from Santa Cruz (sc-156079) or Ambion (ID no 55585). Non-induced or PC12 cells induced to express mutant ATXN7 for 9 days were grown in 6-well plates and transfected at 50–80% confluency using Lipofectamine RNAiMAX transfection reagent (Invitrogen) and a final siRNA concentration of 50 nM according to the manufacturer's instructions.

When indicated, cells were treated with the following chemicals all from Sigma Aldrich; rotenone (0–80 μM), 3-nitropropionic acid (3-NP) (0–10 mM), antimycin A (0–200 nm), sodium azide (NaN_3) (0–70 mM), oligomycin (0–100 μM), vitamine E (α-tocopherol) (1 μM), and apocynin (50 μM). Nutlin-3 (0–10 μM) and ML171 (0–10 μM) were purchased from VWR and EMD Millipore respectively.

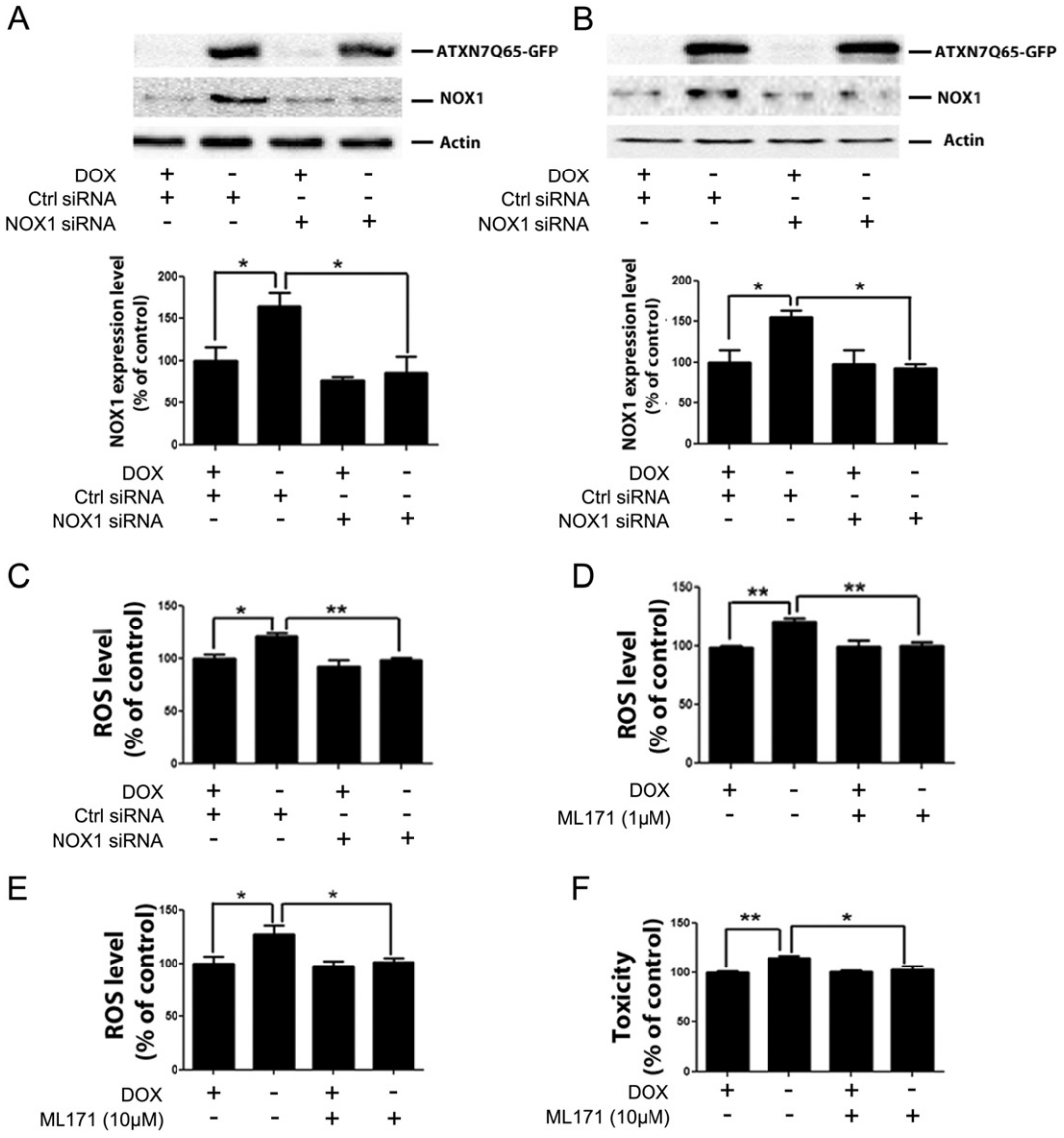

Fig. 2. NOX1 inhibition reduces the ROS level and restores viability in mutant ATXN7 cells. (A) Expression analysis of the 75 kDa NOX1 form in non-induced (+Dox) or FLQ65 cells induced (−Dox) to express ATXN7Q65-GFP for 12 days and treated with control or NOX1 siRNA. (B) Western blot analysis of the 65 kDa NOX1 form in FLQ65 cells grown and treated as in A. (C) Total cellular ROS levels measured by DCHF-DA in FLQ65 cells grown and treated as in A. (D) Total ROS in cells grown as in A, but treated with 1 μM ML171. (E) Total ROS in cells grown as in A, but treated with 10 μM ML171. (F) Toxicity measured by membrane leakage assay, in non-induced (+Dox) or FLQ65 cells induced (−Dox) to express ATXN7Q65-GFP for 12 days while growing in media with or without 10 μM ML171. All data are shown as means ± SEM from three independent experiments. Dox: doxycycline. * $p < 0.05$, ** $p < 0.01$, *** $p < 0.001$.

2.3. Cell lysis, filter trap assay and western blotting

Cell lysis, filter trap and western blotting were done as previously described [9,27]. In brief, cells were lysed with RIPA buffer (Millipore) and following centrifugation at 21,000 ×*g* the soluble fractions, i.e. the supernatants, were collected. To obtain insoluble fractions, pellets were resuspended in DNase I buffer and DNase I treated for 1 h. SDS and DTT were then added to a final concentration of 2% and 100 mM, respectively. The protein concentrations in soluble and insoluble fractions (before SDS and DTT addition) were measured using Bradford assay (Bio-Rad). Soluble or insoluble fractions were then analyzed by western blot and filter trap analysis, respectively. Western blot and filter trap assay membranes were blocked and then probed with primary antibodies at the following concentrations: Ataxin-7 1:700 [7,28], actin 1:500 (sc-1616, Santa Cruz), LDH 1:200 (sc-33781, Santa Cruz), NOX1 1:1000 (SAB4200097, Sigma), NOX1 1:500 (ab131088, Abcam), NOX2 1:200 (sc-74514, Santa Cruz) and p53 1:700 (SC-1313, Santa Cruz). After secondary antibody incubation, the protein of interest was visualized using SuperSignal West Pico or SuperSignal West extended duration substrates (Pierce) and the ChemiDoc XRS + imaging system (BioRad). The signal intensities of protein bands or dots were quantified by Image Lab software (BioRad). For western blotting intensities were normalized against actin or tubulin and the quota for the control sample set to 100%. For filter trap analysis intensities were normalized against the protein concentrations.

2.4. Toxicity measurements

Toxicity was measured by analysis of plasma membrane leakage using the CytoTox-ONE™ assay from Promega as previously described [9]. Briefly, 50,000 induced or non-induced PC12 cells were seeded in 12-well cell culture plates 24 h before measurements. Following drug treatment, 50 μl of cell culture media was transferred into 96 well plates and incubated at room temperature (RT) for 20 min. One hundred microliters of CytoTox-ONE reagent was added to each sample and fluorescence was measured using a Flex station II plate reader at an excitation wavelength of 560 nm and an emission wavelength of 590 nm.

2.5. Determination of mitochondria membrane potential and oxygen consumption

To evaluate the mitochondria membrane potential (Δψm), 20,000 induced or non-induced, treated or non-treated FLQ10 or FLQ65 PC12 cells were seeded in 96-well cell culture plates. Twenty-four hours later the medium was removed, cells were washed and fresh medium containing 10 nM of the fluorescent probe tetramethylrhodamine

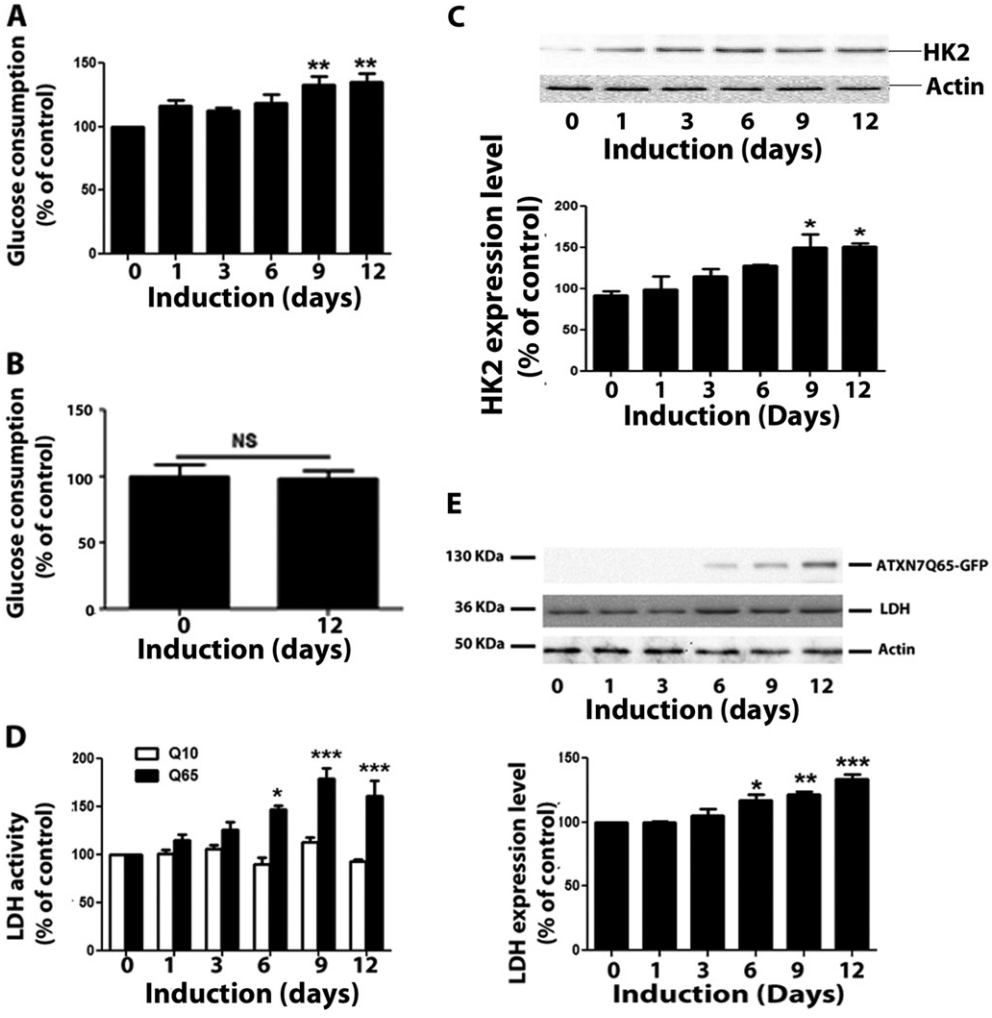

Fig. 3. Expression of ATXN7Q65-GFP results in increased glycolytic activity. (A) Analysis of glucose consumption in FLQ65 cells induced to express mutant ATXN7 for 0, 1, 3, 6, 9, and 12 days, respectively. (B) Glucose consumption in FLQ10 control cells induced to express wild-type ATXN7 for 0 or 12 days. (C) Analysis of hexokinase 2 (HK2) expression in FLQ65 cells induced to express mutant ATXN7 for the indicated number of days. (D) Intracellular LDH activity in FLQ10 and FLQ65 cells induced to express wild-type or mutant ATXN7-GFP for 0–12 days. (E) Analysis of LDH expression in FLQ65 cells grown and treated as in C. For western blots, actin was used for normalizations. All data are shown as means ± SEM from three independent experiments.* $p < 0.05$, ** $p < 0.01$, *** $p < 0.001$.

ethyl ester (TMRE) (Sigma) was added and the plate was incubated for 1 h at 37 °C in the dark. Fluorescence was then measured at 550 nm excitation and 580 nm emission wavelengths using a Flex station II plate reader.

To measure the oxygen consumption, FLQ65 cells non-induced or induced for 12 days, were seeded into 96-well plates at 4×10^4 cells/well. The following day oxygen consumption was performed according to the manufacturer's protocol (600800, Cayman chemicals). Fluorescence was measured at 380 nm excitation and 650 nm emission wavelengths using a Flex station II plate reader. After the oxygen consumption assay, the protein concentration in each well was determined using Lowry assay (Bio-Rad) and the oxygen consumption was normalized against the protein concentration. The value obtained from the untreated non-induced sample was set to 100%.

2.6. Measurement of intracellular LDH activity

Intracellular lactate dehydrogenase (LDH) activity was measured using CytoTox-ONE reagent (Promega). Briefly 50,000 seeded induced or non-induced cells were lysed with 0.2% Triton X-100 (Sigma) and extracts were collected after centrifugation at 12,500 *g* for 10 min. Fifty microliters of extracts was transferred to 96 well plates and incubated at RT for 20 min before 100 μl of CytoTox-ONE reagent was added and fluorescence was measured using a flex station II plate reader at an excitation wavelength of 560 nm and an emission wavelength of 590 nm.

2.7. Glucose consumption and lactate level analysis

Glucose consumption and lactate levels were analyzed using the glucose assay and lactate assay kits from Sigma, following the instructions from the manufacturer. For both assays, 1×10^6 induced or non-induced FLQ10 or FLQ65 cells were seeded in 6 well plates and fresh media were added. Two days later the remaining glucose level in the media was determined for each well and the glucose consumption was calculated as the difference between the amounts of glucose in the fresh media and the detected glucose levels after 48 hours.

For lactate level analysis, the cells were lysed with lactate assay buffer. The extracts were centrifuged at 13,000 ×*g* for 10 min and 50 μl of the extract was taken into a 96 well plate and incubated at RT for 20 min. Fifty microliters of reconstituted lactate assay reagent was then added and incubated in the dark for 30 min at RT after which absorbance was measured at 570 nm. Absorbance values were normalized with the protein concentration.

2.8. Measurement of ATP

ATP was measured using the ATP assay kit (Sigma). Briefly, 1×10^6 induced or non-induced FLQ10 or FLQ65 cells were seeded in 6 well plates 48 h before the assay. On the day of analysis the cells were washed two times in PBS and then lysed with ATP release reagent. Hundred microliters of lysate from each well was then transferred to an opaque 96 well plate and 100 μl ATP assay mix working solution was

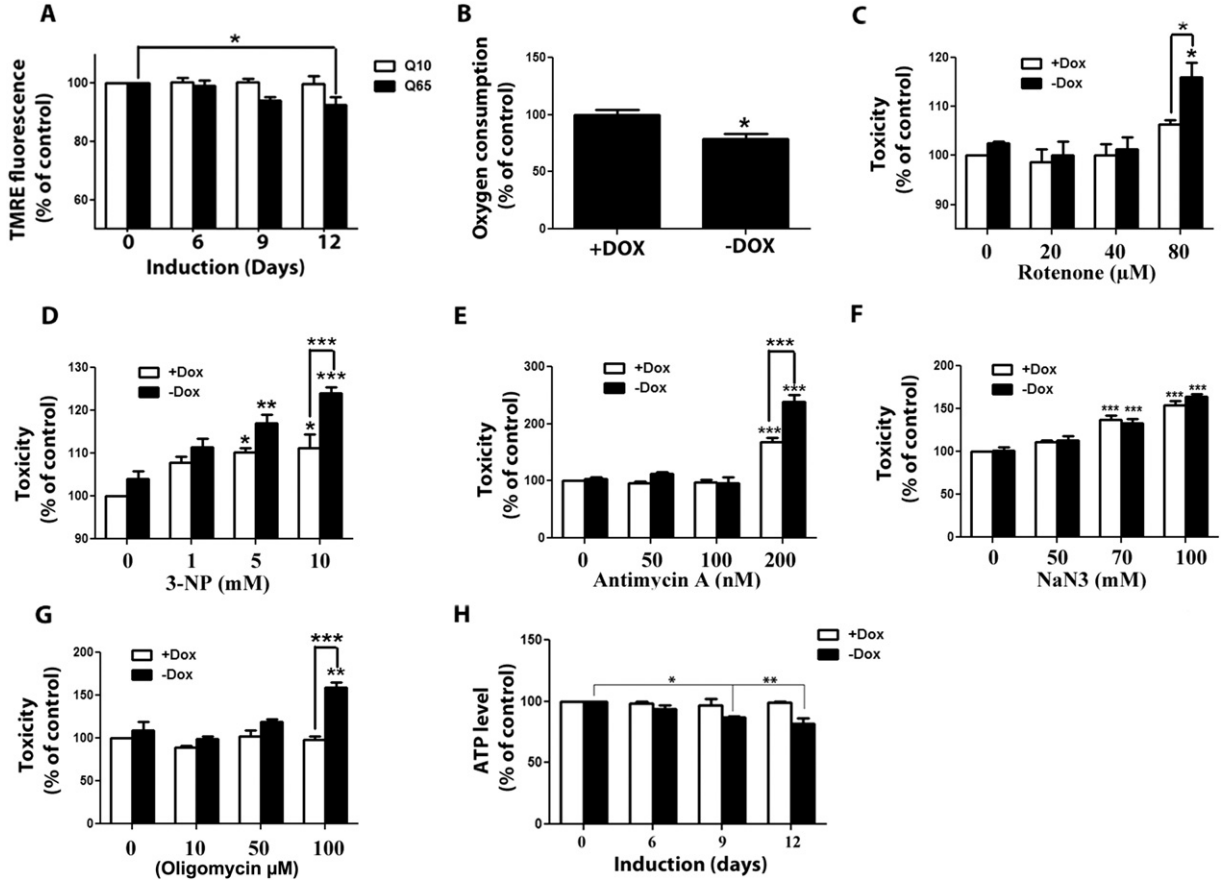

Fig. 4. Mitochondrial respiratory chain impairment in mutant ATXN7 cells. (A) Mitochondrial membrane potential measured by TMRE in FLQ10 or FLQ65 cells induced to express wild-type (Q10) or mutant (Q65) ATXN7 for 0, 6, 9, and 12 days, respectively. (B) Oxygen consumption in non-induced (+Dox) and 12 days induced (−Dox) FLQ65 cells expressing mutant ATXN7. (C) Toxicity in non-induced (+Dox) and FLQ65 cells induced (−Dox) to express ATXN7Q65-GFP for 6 days and treated with the mitochondrial complex I inhibitor rotenone for 12 h, (D) toxicity in cells grown as in B, but treated with the complex II inhibitor 3-NP, (E) toxicity in cells grown as in B, but treated with the complex III inhibitor antimycin A, (F) toxicity in cells grown as in B, but treated with the complex IV inhibitor NaN3, and (G) toxicity in cells grown as in B, but treated with the complex V inhibitor oligomycin. (H) The total ATP level in FLQ10 or FLQ65 cells induced to express wild-type or mutant ATXN7 for 0, 6, 9, and 12 days, respectively. Dox: doxycycline. All data are shown as means ± SEM from three independent experiments.* $p < 0.05$, ** $p < 0.01$, *** $p < 0.001$.

added to each well before the luminescence was measured immediately using a micro-plate luminometer (Promega). The obtained luminescence values were normalized by protein concentration, and the value obtained from non-induced sample was set to 100%.

2.9. RNA purification and reverse transcription–polymerase chain reaction

The mRNA expression of NOX1, NOX2, GLUT1, AIF, and TIGAR was evaluated by the semi-quantitative RT-PCR method. RNA from non-induced and 12-day induced FLQ65 cells was purified using the GeneJet RNA purification kit (#KO731, Thermo Scientific). Two thousand nanograms of total RNA was used for RT-PCR using RevertAid H minus First strand cDNA synthesis kit (#K1631, Thermo Scientific). Transcribed mRNAs in each sample were amplified using validated rat primers from Qiagen or Santa Cruz for rat ACTIN, GAPDH, NOX1, NOX2, NOX4, GLUT1, AIF, and TIGAR and quantified at individual cycle number for each transcript using a ChemiDoc XRS + imaging system (Bio-Rad) and the Image Lab software (Bio-Rad). Actin mRNA levels were used for normalizations.

2.10. Statistical analysis

Statistical analyses were done by one-way ANOVA followed by Tukey's post-hoc test using Prism graph pad 5.0.

3. Results

3.1. NOX1 expression and activity are increased in mutant ATXN7 cells

We have previously shown that expression of mutant ATXN7 (ATXN7Q65-GFP) in a stable inducible SCA7 PC12 cell model (FLQ65) results in increased ROS production by NADPH oxidases, oxidative stress and toxicity [9]. To determine which specific NOX member(s) that is involved in the mutant ATXN7 induced toxicity, we analyzed the expression of different NOX members in our SCA7 model. The results showed that both NOX1 and NOX2 are expressed in PC12 cells (Fig. 1). However, upon induction of mutant ATXN7 expression, by the removal of doxycycline (Dox) from the media, the NOX1 mRNA level was up-regulated approximately 6 times, whereas the NOX2 level remained unchanged (Fig. 1A). Analysis of NOX1 protein levels with western blot resulted in detection of two different sized NOX1 protein forms, one of around 65 kDa, primarily detected by an antibody from Abcam (Fig. 1B), and a 75 kDa form, primarily detected using an antibody from Sigma (Fig. 1C). Both NOX1 forms were increased, between 1.5 and 10 times, upon induction of mutant ATXN7 (Fig. 1B–C), and the increase of both forms was specifically down-regulated by siRNA directed against rat NOX1 (Fig. 2A–B). In contrast, induction of mutant ATXN7 had no effect on the level of NOX2 protein (Fig. 1E). Furthermore, induction of ATXN7 with a non-disease causing repeat of 10 glutamines (ATXN7Q10-GFP) in FLQ10 control cells did not alter either the NOX1 or NOX2 expression (Fig. 1D and F).

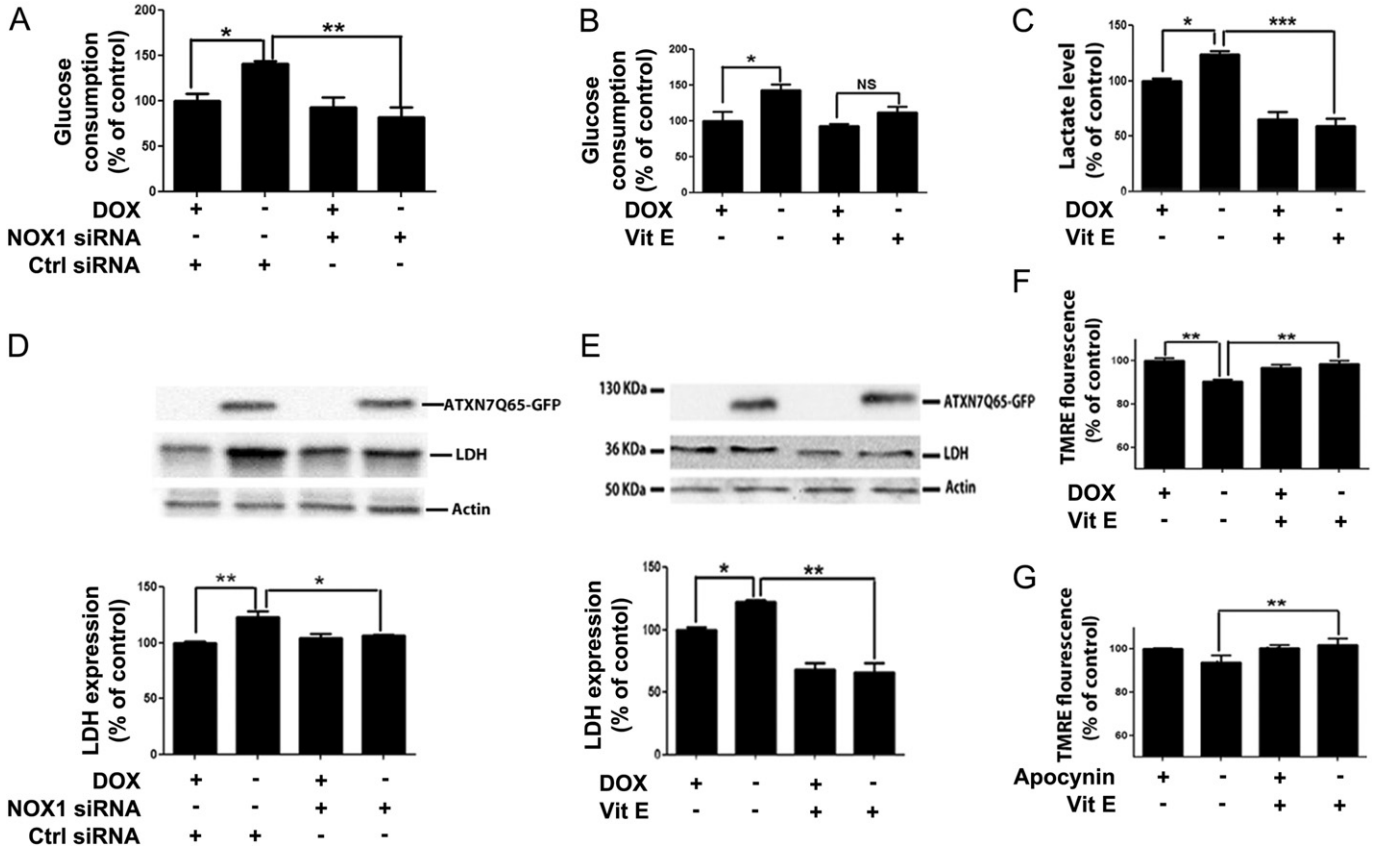

Fig. 5. NOX1 inhibition or ROS scavenging reverses the mutant ATXN7 induced metabolic shift. (A) Glucose consumption in non-induced (+Dox) or FLQ65 cells induced (−Dox) to express mutant ATXN7 for 12 days and treated with control or NOX1 siRNA. (B) Glucose consumption in cells grown as in A, but treated with 1 μM of the ROS scavenger vitamin E (Vit E). (C) Lactate levels in FLQ65 cells grown and treated as in B. (D) LDH expression in FLQ65 cells grown and treated with NOX1 siRNA as in A. (E) LDH expression in FLQ65 cells grown and treated with Vit E as in B. (F) Mitochondria membrane potential in FLQ65 cells grown and treated with Vit E as in B. (F) Mitochondria membrane potential in non-induced (+Dox) or FLQ65 cells induced (−Dox) to express mutant ATXN7 for 12 days while growing in media with or without 50 μM Apocynin. Actin was used as loading control for quantifications in western blots. Data are shown as means ± SEM from three independent experiments. Dox: doxycycline. * $p < 0.05$, ** $p < 0.01$, *** $p < 0.001$.

To confirm that the observed up-regulation of NOX1 is the source of the increased ROS generation in SCA7 cells, we measured the ROS levels in FLQ65 cells following NOX1 knock-down or inhibition. As expected, NOX1 siRNA, as well as treatment with the NOX1 inhibitor ML171, which has a greater than 30-fold selectivity for NOX1 over other NOX isoforms [29], completely reversed the ~25% ROS increase in ATXN7Q65-GFP expressing cells (Fig. 2C–E). Furthermore, inhibition of NOX1 also ameliorated the mutant ATXN7 toxicity (Fig. 2F). Taken together, these results suggest that mutant ATXN7 causes increased ROS levels and oxidative stress by up-regulation and activation of the NOX1 enzyme.

3.2. ATXN7Q65-GFP expression results in metabolic dysregulation and reduced ATP levels

NOX1 activity was recently linked to regulation of the balance between glycolysis and mitochondrial respiration [30–32]. Next, we therefore investigated the glycolytic activity by measuring the glucose consumption, the expression level of hexokinase 2 (HK2), as well as the LDH activity and expression in SCA7 cells. A clear gradual increase in glucose consumption (Fig. 3A), HK2 expression (Fig. 3C), intracellular LDH activity (Fig. 3D) and LDH expression (Fig. 3E) could be detected from six days onwards after induction of mutant ATXN7 in FLQ65 cells. Twelve days after induction an approximate 30–40% increase in glucose consumption and a 30–50% increase in HK2, as well as LDH expression and activity, could be observed. In addition, a 25% increase in the lactate level could be observed in mutant ATXN7 cells (Fig. 5C). In contrast, induction of wild-type ATXN7 in FLQ10 control cells had no effect on glucose consumption, HK2 or LDH (Fig. 3B, D and data not shown).

To determine the status of the electron transport chain (ETC.) and mitochondrial respiration in SCA7 cells, we next analyzed the mitochondria membrane potential ($\Delta\psi m$) and the oxygen consumption. In FLQ65 cells induced to express mutant ATXN7 the $\Delta\psi m$ was gradually decreased from day 9 onwards (Fig. 4A), whereas induction of wild-type ATXN7 had no effect on the $\Delta\psi m$ (Fig. 4A). Oxygen consumption was also significantly reduced by approximately 20% in mutant ATXN7 expressing cells (Fig. 4B). To further confirm the negative effect of mutant ATXN7 on mitochondrial ETC. function we also, as previously done in HD polyglutamine disease models, assessed the sensitivity of control and induced FLQ65 cells to inhibitors of mitochondria complexes I, II, III, IV and V [20,33]. The experiments were performed six days after induction, when expression of mutant ATXN7 by itself has not yet induced toxicity (Fig. 4C–G). However, at this early time-point treatment with

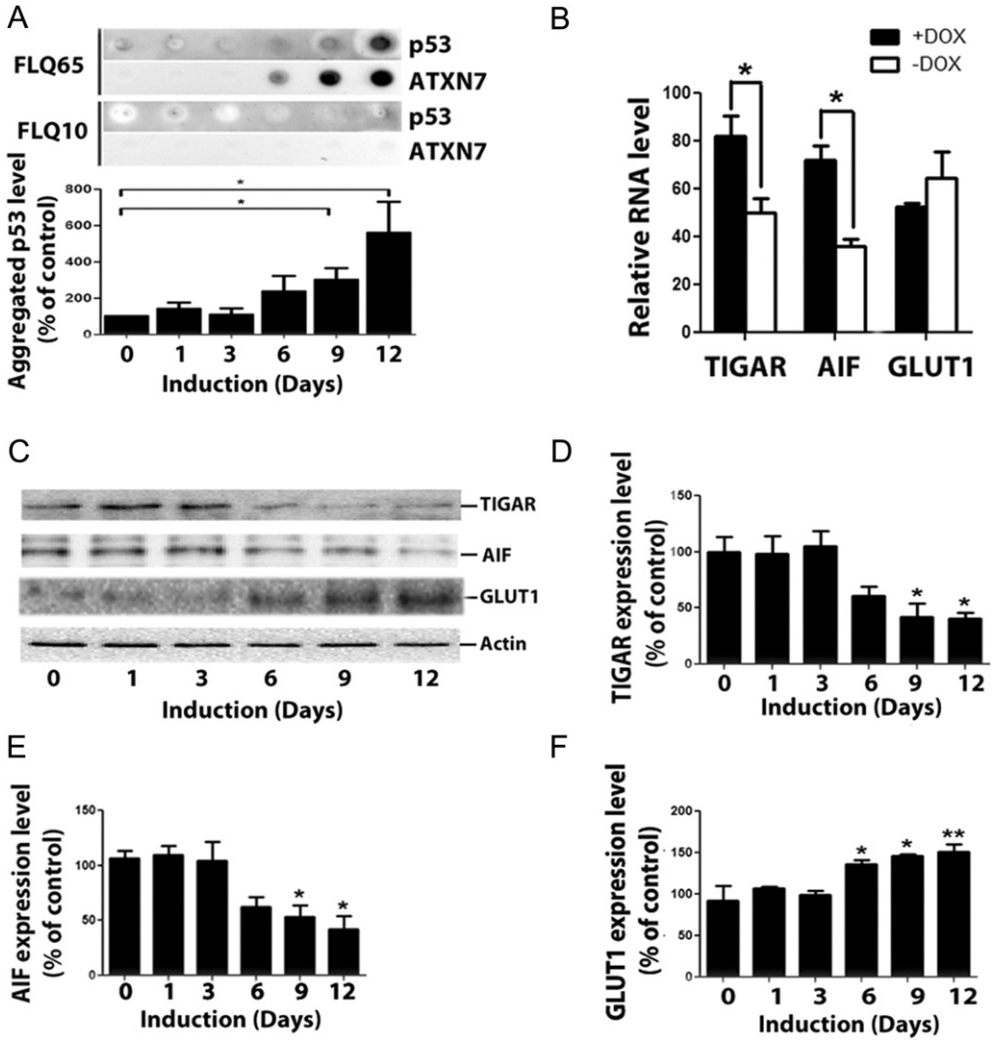

Fig. 6. The p53 transcriptional regulation of metabolic genes is altered in SCA7 cells. (A). Analysis of p53 and ATXN7 co-aggregation in FLQ10 or FLQ65 induced to express ATXN7Q10-GFP or ATXN7Q65-GFP for the indicated number of days. Aggregated ATXN7 and p53 were collected and analyzed by cell fractionation and filter trap assay. (B) Analysis of TIGAR, AIF and GLUT1 mRNA levels in non-induced (+Dox) or FLQ65 cells induced (−Dox) to express mutant ATXN7 for 12 days. The mRNA levels of actin were used for normalization. (C). Western blot analysis of TIGAR, AIF and GLUT1 protein levels in FLQ65 cells induced to express ATXN7Q65-GFP for the indicated number of days. (D). Quantification of the TIGAR expression level. (E). Quantification of the AIF expression level. (F). Quantification of the GLUT1 expression level. For western blot quantifications, actin was used for normalizations. Dox: doxycycline. Data are shown as means ± SEM from three independent experiments. * $p < 0.05$, ** $p < 0.01$, *** $p < 0.001$.

complex I, II, III and V inhibitors all resulted in 10–70% more toxicity in mutant ATXN7 expressing cells, compared to non-induced control cells (Fig. 4C–G), indicating that the electron transport chain is compromised by mutant ATXN7. Interestingly, mutant ATXN7 did not sensitize cells towards complex IV inhibition (Fig. 4F).

To analyze whether the observed metabolic changes had an effect on the energy level in SCA7 cells, we next analyzed the ATP levels in non-induced and induced FLQ10 and FLQ65 cells. A gradual decrease of the ATP level was observed upon induction of mutant ATXN7 in FLQ65 cells, and twelve days after induction the ATP level was decreased by 20% (Fig. 4H). In contrast, no change in the ATP levels could be observed in FLQ10 cells expressing wild-type ATXN7 at any time point (Fig. 4H).

3.3. NOX inhibition or ROS scavenging reverses the mutant ATXN7 induced metabolic dysregulation

To establish if the increased NOX1 activity in mutant ATXN7 cells is required for promoting the observed metabolic dysfunction, we next investigated whether the metabolic status could be restored by NOX1 knock-down or scavenging of NOX1 produced ROS. Indeed, the increase in glucose consumption (Fig. 5A–B), lactate (Fig. 5C) and LDH levels (Fig. 5D–E), as well as the decrease in mitochondrial membrane potential (Fig. 5F–G) could all be reversed by NOX1 knock-down or ROS scavenging.

To verify that the metabolic dysfunction induced by mutant ATXN7 is not specific to the inducible SCA7 PC12 cell model, we transiently transfected human HeLa cells with ATXN7 expression constructs and analyzed the NOX1 level, as well as the metabolic status 72 h later. Also in this SCA7 model, expression of mutant full-length (FLQ65) or truncated (TrQ65) ATXN7 resulted in a small approximately 10% increase in NOX1 expression, compared to control cells expressing wild-type ATXN7 (Supplementary Fig. S1). Moreover, the small increase in NOX1 was associated with increased glycolytic activity, evident by for instance an approximate 20% increase in glucose consumption and LDH expression in HeLa cells (Supplementary Fig. S1).

3.4. Altered p53 function contributes to the metabolic dysfunction

The p53 protein is a key regulator of cellular metabolism. Using the same stable inducible SCA7 model as in this study, we have previously shown that p53 co-aggregates with mutant ATXN7 and that this reduces the soluble p53 level and transcriptional activity [27]. Consistent with this, we could again in induced FLQ65 cells detect p53 in the insoluble cell fractions containing mutant ATXN7 aggregates; see Fig. 6A.

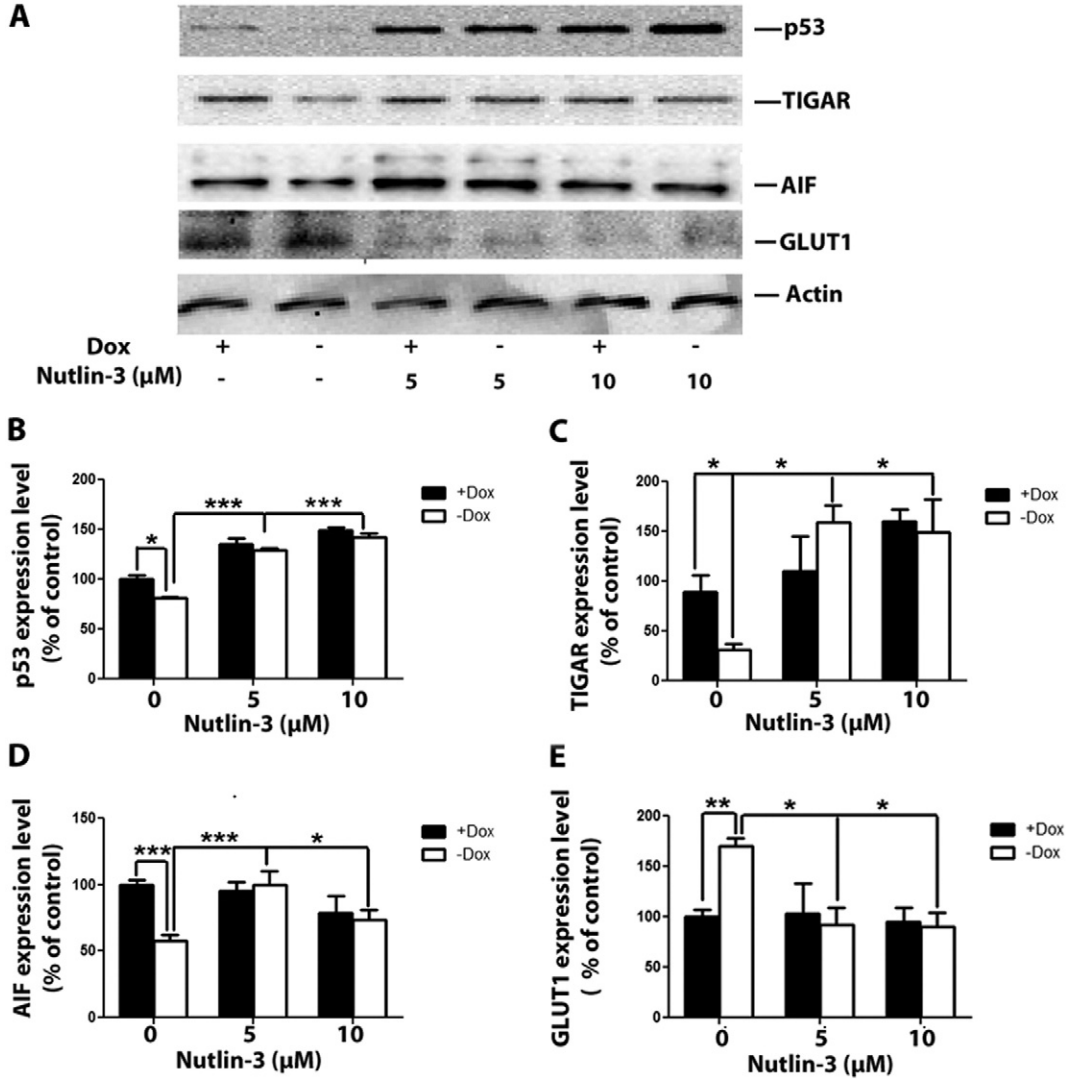

Fig. 7. Nutlin-3 treatment restores the p53-mediated regulation of metabolic proteins. (A). Western blot analysis of p53, TIGAR, AIF and GLUT1 expression in non-induced (+Dox) or 12 days induced (−Dox) FLQ65 cells grown in media with or without nutlin-3 (0–10 μM). (B). Quantification of the p53 expression level. (C). Quantification of the TIGAR expression level. (D). Quantification of the AIF expression level. (E). Quantification of the GLUT1 expression level. Actin was used for normalization prior to quantification. Data are shown as means ± SEM from three independent experiments. Dox: doxycycline. * $p < 0.05$, ** $p < 0.01$, *** $p < 0.001$.

Furthermore, an approximate 20% decrease in the soluble p53 level was again detected in SCA7 cells; see Fig. 7A–B. In contrast, no detection of p53 in the insoluble fraction or change of soluble p53 levels, could be observed in FLQ10 control cells induced to express wild-type ATXN7 (Fig. 6A and data not shown).

To investigate whether the altered p53 level contributes to the metabolic dysfunction in SCA7, we analyzed the expression of some key metabolic genes/proteins, positively (TIGAR and AIF) or negatively (GLUT1), regulated by p53 on the transcriptional level. Consistent with the reduced soluble p53 levels, we could detect a significant 30% decrease of TIGAR and AIF mRNA, as well as a small, but non-significant, increase in GLUT1 mRNA in mutant ATXN7 cells (Fig. 6B). In agreement with the mRNA results, the protein levels of TIGAR and AIF were gradually decreased, while a gradual increase in GLUT1 was observed following induction of mutant ATXN7 in FLQ65 cells (Fig. 6C–F). In fact, twelve days after induction TIGAR, AIF and GLUT1 protein levels were all changed by approximately 50%.

To further reassert the role of p53 dysfunction, we next investigated whether increasing the p53 levels could reverse the mutant ATXN7 induced metabolic alterations. Indeed, nutlin-3 treatment, which increased the p53 level by approximately 50% (Fig. 7A–B), not only restored the expression levels of TIGAR, AIF and GLUT1 (Fig. 7A–E), but also reversed the metabolic dysregulation. This was evident by for instance the restoration of glucose consumption (Fig. 8A) and the LDH expression level (Fig. 8B–D). Interestingly, enhancing p53 levels also prevented the up-regulation of NOX1 expression in mutant ATXN7 cells (Fig. 8B–C).

4. Discussion

Metabolic dysfunction has been implicated in the pathology of SCA7 [1,19,22]. However, the exact molecular mechanism(s) underlying this pathological change have not been established. In this study, we therefore set out to investigate how mutant ATXN7 affects cellular metabolism and found that the mutant protein caused mitochondrial dysfunction, metabolic imbalance and reduced ATP production by disrupting p53 and NOX1 activities.

The p53 transcription factor is a major regulator of cellular metabolism. In SCA7 cells, we could show that p53 co-aggregates with mutant ATXN7 and the soluble p53 levels and the p53 transcriptional activity is thus reduced (Figs. 6–7). In turn, this resulted in a more than 50% decrease in the level of some key p53-regulated metabolic proteins like AIF. AIF is essential for the integrity of the mitochondrial ETC. and AIF knock-out mice show mitochondrial abnormalities and reduced respiratory capacity; for review see [34]. Consistent with this, we found that SCA7 cells had reduced ETC. integrity, mitochondrial membrane potential and oxygen consumption (Fig. 4). Loss of AIF function might hence be a key contributor to the mitochondrial abnormalities observed in SCA7 [19]. This is further supported by the fact that loss of AIF in mice results in neurodegeneration and death of primarily cerebellar and retinal neurons, the neuronal types mostly affected in SCA7 disease [34].

In addition to promoting mitochondrial respiration, p53 also inhibits glycolysis under normal conditions. This is achieved through induction of TIGAR and negative regulation of GLUT expression [23,24]. In SCA7 cells, the reduced p53 function resulted in 50% lower TIGAR and 40% higher GLUT1 expression and thus an increased glycolytic activity (Fig. 6). This was evident by an increased glucose consumption, HK2 and LDH expression, as well as LDH activity in SCA7 cells (Fig. 3). Increasing the p53 activity in SCA7 cells, not only restored the expression of AIF, TIGAR and GLUT1, but also reversed the metabolic disruption (Figs. 7–8). Taken together, our results show that the mutant ATXN7 induced p53 dysregulation causes a metabolic imbalance with decreased respiratory capacity and an increased reliance on glycolysis for energy production. As a consequence the ATP levels were reduced by 20% in SCA7 cells (Fig. 4).

Enhanced activation of the NOX1 enzyme was recently shown to be critical in supporting elevated glycolysis in cancer cells suffering from mitochondrial respiratory defect [30]. In agreement with this, we found that the reduced respiration in SCA7 cells was coupled with a significant up-regulation of NOX1 on both the mRNA and protein level

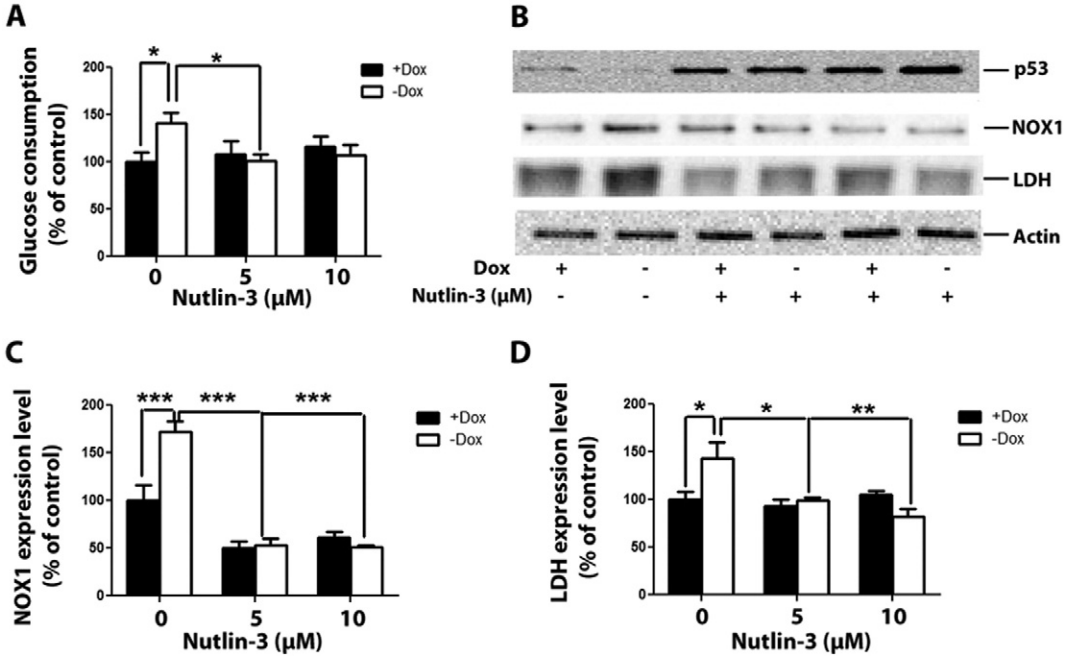

Fig. 8. Enhancement of the p53 level reverses the metabolic shift in mutant ATXN7 cells. (A) Glucose consumption in non-induced (+Dox) or 12 days induced (−Dox) FLQ65 cells grown in media with or without nutlin-3 (0–10 μM). (B) Western blot analysis of NOX1 and LDH expression in cells grown and treated as in A. (C) Quantification of the 75 kDa NOX1 protein expression. (D) Quantification of the LDH expression. Actin was used for normalization prior to quantification. Dox: doxycycline. Data are shown as means ± SEM from three independent experiments. * $p < 0.05$, ** $p < 0.01$, *** $p < 0.001$.

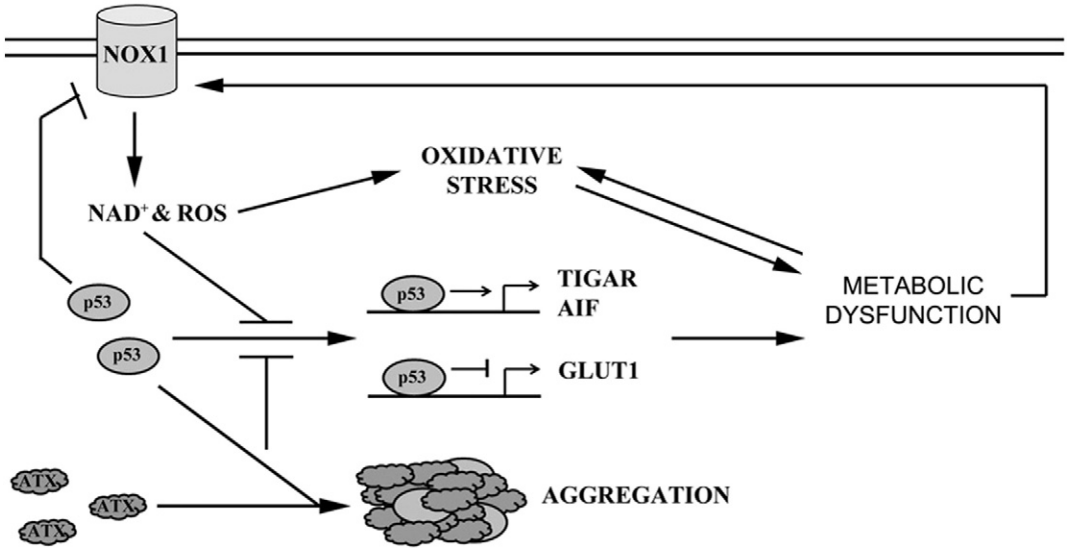

Fig. 9. Proposed model of mutant ATXN7 induced metabolic dysfunction and oxidative stress. p53-mutant ATXN7 co-aggregation and NOX1-mediated inactivation of p53 results in reduced p53-mediated transcriptional regulation of essential metabolic proteins, including TIGAR, AIF and GLUT1. In turn this results in reduced mitochondrial function and ATP production. NOX1 activity is induced in response to the increased dependence on glycolysis and potentially also through decreased negative regulation by p53. The enhanced ROS production from NOX1 results in oxidative stress and further reduction of p53 function.

(Fig. 1). Furthermore, we could show that the increased NOX1 activity was required for the metabolic dysregulation in SCA7 cells, as knock-down or inhibition of NOX1 reversed the metabolic phenotype (Fig. 2). Interestingly, two forms of NOX1, one of the predicted 65 kDa size and another larger form of ~75 kDa, were detected and found to be increased in SCA7 cells. The 75 kDa NOX1 form has previously been reported in rat cells and suggested to be a post-translationally modified form of NOX1 [35].

How NOX1 activity supports the metabolic dysregulation in SCA7 cells is still largely unclear. However, NAD + generated by NOX1 during ROS production could activate SIRT1, resulting in enhanced p53 deacetylation and reduced p53 transcriptional activity [36]. Furthermore, p53 contain redox sensitive thiol groups which could be modified by ROS generated from NOX1 [37,38]. In fact, the metabolic dysregulation in SCA7 cells could be blocked, not only by NOX1 knock-down, but also by ROS scavenging, suggesting that the NOX1 generated ROS is indeed essential for the metabolic dysregulation (Fig. 5). It is thus tempting to speculate that the increased NOX1 activity could result in p53 inactivation, which together with the p53-ATXN7 co-aggregation, synergistically would cause a reduction in soluble transcriptional active p53 able to regulate AIF, TIGAR and GLUT1 expression. Interestingly, we could also observe that upon increasing the p53 activity in SCA7 cells, NOX1 expression was normalized (Fig. 8), suggesting that p53 might in turn negatively control the NOX1 expression. Taken together, this could thus create a feed-forward loop (Fig. 9), where p53-ATXN7 co-aggregation and NOX1-mediated p53 inactivation result in reduced p53 transcriptional activity, metabolic dysregulation and further NOX1 activity, as well as oxidative stress. In fact, we have shown that breaking this proposed cycle, through blockage of p53-ATXN7 co-aggregation [27], increasing p53 levels (Figs. 7–8), as well as inhibiting NOX1 activity or ROS scavenging (Fig. 5) ameliorate the mutant ATXN7 induced dysfunction.

In conclusion, we have identified a novel mechanism in which mutant ATXN7 by disrupting p53 function and inducing NOX1 activity results in metabolic dysregulation, reduced ATP levels, oxidative stress and toxicity. Our results not only enhance the understanding of mechanisms causing metabolic dysfunction and toxicity in SCA7 disease, but also identify NOX1 as a novel potential therapeutic target in SCA7 and possibly other polyQ diseases.

Supplementary data to this article can be found online at http://dx.doi.org/10.1016/j.bbabio.2015.01.012.

Conflicts of interest

Neither of the authors, Ajayi Abiodun, Xin Yu, Carolina Wahlo-Svedin, Galateia Tsirigotaki, Victor Karlström or Anna-Lena Ström, have any conflicts of interest to report in regards to the manuscript entitled Altered p53 and NOX1 activity causes bioenergetic defects in a SCA7 polyglutamine disease model.

Acknowledgment

This work was supported by the Swedish Research Council (90274201), Harald Jeanssons stiftelse, Harald och Greta Jeanssons stiftelse, Magn Bergvalls stiftelse, O.E. och Edla Johanssons vetenskapliga stiftelse, Åhlen stiftelsen, Längmanska kulturfonden, Sigurd och Elsa Goljes stiftelse and The Swedish Association of Persons with Neurological Disabilities.

References

[1] P.O. Bauer, N. Nukina, The pathogenic mechanisms of polyglutamine diseases and current therapeutic strategies, J. Neurochem. 110 (2009) 1737–1765.
[2] G.A. Garden, A.R. La Spada, Molecular pathogenesis and cellular pathology of spinocerebellar ataxia type 7 neurodegeneration, Cerebellum 7 (2008) 138–149.
[3] C. Yanicostas, E. Barbieri, M. Hibi, A. Brice, G. Stevanin, N. Soussi-Yanicostas, Requirement for zebrafish ataxin-7 in differentiation of photoreceptors and cerebellar neurons, Plos One 7 (2012).
[4] D. Helmlinger, S. Hardy, S. Sasorith, F. Klein, F. Robert, C. Weber, L. Miguet, N. Potier, A. Van-Dorsselaer, J.M. Wurtz, J.L. Mandel, L. Tora, D. Devys, Ataxin-7 is a subunit of GCN5 histone acetyltransferase-containing complexes, Hum. Mol. Genet. 13 (2004) 1257–1265.
[5] Y. Nakamura, K. Tagawa, T. Oka, T. Sasabe, H. Ito, H. Shiwaku, A.R. La Spada, H. Okazawa, Ataxin-7 associates with microtubules and stabilizes the cytoskeletal network, Hum. Mol. Genet. 21 (2012) 1099–1110.
[6] V.B. Palhan, S. Chen, G.H. Peng, A. Tjernberg, A.M. Gamper, Y. Fan, B.T. Chait, A.R. La Spada, R.G. Roeder, Polyglutamine-expanded ataxin-7 inhibits STAGA histone acetyltransferase activity to produce retinal degeneration, Proc. Natl. Acad. Sci. U. S. A. 102 (2005) 8472–8477.
[7] J. Jonasson, A.L. Strom, P. Hart, T. Brannstrom, L. Forsgren, M. Holmberg, Expression of ataxin-7 in CNS and non-CNS tissue of normal and SCA7 individuals, Acta Neuropathol. 104 (2002) 29–37.
[8] A. Ajayi, X. Yu, A.L. Strom, The role of NADPH oxidase (NOX) enzymes in neurodegenerative disease, Front. Biol. 8 (2013) 175–188.
[9] A. Ajayi, X. Yu, S. Lindberg, U. Langel, A.L. Strom, Expanded ataxin-7 cause toxicity by inducing ROS production from NADPH oxidase complexes in a stable inducible spinocerebellar ataxia type 7 (SCA7) model, BMC Neurosci. 13 (2012) 86.
[10] A. Bertoni, P. Giuliano, M. Galgani, D. Rotoli, L. Ulianich, A. Adornetto, M.R. Santillo, A. Porcellini, V.E. Avvedimento, Early and late events induced by polyQ-expanded proteins: identification of a common pathogenic property of polyQ-expanded proteins, J. Biol. Chem. 286 (2011) 4727–4741.

[11] P.D. Maldonado, E. Molina-Jijon, J. Villeda-Hernandez, S. Galvan-Arzate, A. Santamaria, J. Pedraza-Chaverri, NAD(P)H oxidase contributes to neurotoxicity in an excitotoxic/prooxidant model of Huntington's disease in rats: protective role of apocynin, J. Neurosci. Res. 88 (2010) 620–629.
[12] A. Valencia, E. Sapp, J.S. Kimm, H. McClory, P.B. Reeves, J. Alexander, K.A. Ansong, N. Masso, M.P. Frosch, K.B. Kegel, X. Li, M. DiFiglia, Elevated NADPH oxidase activity contributes to oxidative stress and cell death in Huntington's disease, Hum. Mol. Genet. 22 (2013) 1112–1131.
[13] H.M. Gao, H. Zhou, J.S. Hong, NADPH oxidases: novel therapeutic targets for neurodegenerative diseases, Trends Pharmacol. Sci. 33 (2012) 295–303.
[14] M. Katsuyama, K. Matsuno, C. Yabe-Nishimura, Physiological roles of NOX/NADPH oxidase, the superoxide-generating enzyme, J. Clin. Biochem. Nutr. 50 (2012) 9–22.
[15] C.M. Chen, Mitochondrial dysfunction, metabolic deficits, and increased oxidative stress in Huntington's disease, Chang Gung Med. J. 34 (2011) 135–152.
[16] M.G.V. Heiden, L.C. Cantley, C.B. Thompson, Understanding the Warburg effect: the metabolic requirements of cell proliferation, Science 324 (2009) 1029–1033.
[17] T. Soga, Cancer metabolism: key players in metabolic reprogramming, Cancer Sci. 104 (2013) 275–281.
[18] T.C. Ju, Y.S. Lin, Y. Chern, Energy dysfunction in Huntington's disease: insights from PGC-1alpha, AMPK, and CKB, Cell Mol Life Sci 69 (24) (2012) 4107–4120.
[19] L. Forsgren, R. Libelius, M. Holmberg, U. von Dobeln, R. Wibom, J. Heijbel, O. Sandgren, G. Holmgren, Muscle morphology and mitochondrial investigations of a family with autosomal dominant cerebellar ataxia and retinal degeneration mapped to chromosome 3p12-p21.1, J. Neurol. Sci. 144 (1996) 91–98.
[20] S. Gines, I.S. Seong, E. Fossale, E. Ivanova, F. Trettel, J.F. Gusella, V.C. Wheeler, F. Persichetti, M.E. MacDonald, Specific progressive cAMP reduction implicates energy deficit in presymptomatic Huntington's disease knock-in mice, Hum. Mol. Genet. 12 (2003) 497–508.
[21] M.N. Laco, C.R. Oliveira, H.L. Paulson, A.C. Rego, Compromised mitochondrial complex II in models of Machado–Joseph disease, Biochim. Biophys. Acta 1822 (2012) 139–149.
[22] J. Johansson, L. Forsgren, O. Sandgren, A. Brice, G. Holmgren, M. Holmberg, Expanded CAG repeats in Swedish spinocerebellar ataxia type 7 (SCA7) patients: effect of CAG repeat length on the clinical manifestation, Hum. Mol. Genet. 7 (1998) 171–176.
[23] C.R. Berkers, O.D. Maddocks, E.C. Cheung, I. Mor, K.H. Vousden, Metabolic regulation by p53 family members, Cell Metab. 18 (2013) 617–633.
[24] Y. Liang, J. Liu, Z. Feng, The regulation of cellular metabolism by tumor suppressor p53, Cell Biosci 3 (2013) 9.
[25] X. Yu, A. Ajayi, N.R. Boga, A.L. Strom, Differential degradation of full-length and cleaved ataxin-7 fragments in a novel stable inducible SCA7 model, J. Mol. Neurosci. 47 (2012) 219–233.
[26] A.L. Strom, L. Forsgren, M. Holmberg, A role for both wild-type and expanded ataxin-7 in transcriptional regulation, Neurobiol. Dis. 20 (2005) 646–655.
[27] X. Yu, A. Munoz-Alarcon, A. Ajayi, K.E. Webling, A. Steinhof, U. Langel, A.L. Strom, Inhibition of autophagy via p53-mediated disruption of ULK1 in a SCA7 polyglutamine disease model, J. Mol. Neurosci. 50 (2013) 586–599.
[28] A.L. Strom, J. Jonasson, P. Hart, T. Brannstrom, L. Forsgren, M. Holmberg, Cloning and expression analysis of the murine homolog of the spinocerebellar ataxia type 7 (SCA7) gene, Gene 285 (2002) 91–99.
[29] D. Gianni, N. Taulet, H. Zhang, C. DerMardirossian, J. Kister, L. Martinez, W.R. Roush, S.J. Brown, G.M. Bokoch, H. Rosen, A novel and specific NADPH oxidase-1 (Nox1) small-molecule inhibitor blocks the formation of functional invadopodia in human colon cancer cells, ACS Chem. Biol. 5 (2010) 981–993.
[30] W. Lu, Y. Hu, G. Chen, Z. Chen, H. Zhang, F. Wang, L. Feng, H. Pelicano, H. Wang, M.J. Keating, J. Liu, W. McKeehan, Y. Luo, P. Huang, Novel role of NOX in supporting aerobic glycolysis in cancer cells with mitochondrial dysfunction and as a potential target for cancer therapy, PLoS Biol. 10 (2012) e1001326.
[31] C. Prata, T. Maraldi, D. Fiorentini, L. Zambonin, G. Hakim, L. Landi, Nox-generated ROS modulate glucose uptake in a leukaemic cell line, Free Radic. Res. 42 (2008) 405–414.
[32] H.R. Rezvani, R. Rossignol, N. Ali, G. Benard, X. Tang, H.S. Yang, T. Jouary, H. de Verneuil, A. Taieb, A.L. Kim, F. Mazurier, XPC silencing in normal human keratinocytes triggers metabolic alterations through NOX-1 activation-mediated reactive oxygen species, Biochim. Biophys. Acta 1807 (2011) 609–619.
[33] Q. Ruan, M. Lesort, M.E. MacDonald, G.V. Johnson, Striatal cells from mutant huntingtin knock-in mice are selectively vulnerable to mitochondrial complex II inhibitor-induced cell death through a non-apoptotic pathway, Hum. Mol. Genet. 13 (2004) 669–681.
[34] B.M. Polster, AIF, reactive oxygen species, and neurodegeneration: a "complex" problem, Neurochem. Int. 62 (2013) 695–702.
[35] M. Pleskova, K.F. Beck, M.H. Behrens, A. Huwiler, B. Fichtlscherer, O. Wingerter, R.P. Brandes, A. Mulsch, J. Pfeilschifter, Nitric oxide down-regulates the expression of the catalytic NADPH oxidase subunit Nox1 in rat renal mesangial cells, FASEB J. 20 (2006) 139–141.
[36] R. Puca, L. Nardinocchi, G. Starace, G. Rechavi, A. Sacchi, D. Givol, G. D'Orazi, Nox1 is involved in p53 deacetylation and suppression of its transcriptional activity and apoptosis, Free Radic. Biol. Med. 48 (2010) 1338–1346.
[37] X.Z. Sun, C. Vinci, L. Makmura, S. Han, D. Tran, J. Nguyen, M. Hamann, S. Grazziani, S. Sheppard, M. Gutova, F. Zhou, J. Thomas, J. Momand, Formation of disulfide bond in p53 correlates with inhibition of DNA binding and tetramerization, Antioxid. Redox Signal. 5 (2003) 655–665.
[38] C.S. Velu, S.K. Niture, C.E. Doneanu, N. Pattabiraman, K.S. Srivenugopal, Human p53 is inhibited by glutathionylation of cysteines present in the proximal DNA-binding domain during oxidative stress, Biochemistry 46 (2007) 7765–7780.